Kinetic model for layer-by-layer crystal growth in chain molecules

Alexander Bourque, Gregory C. Rutledge*

Department of Chemical Engineering, Massachusetts Institute of Technology,

Cambridge, MA 02139

*Corresponding author. Tel.: +1 617 253 0171; fax: +1 617 258 5766.

E-mail address: rutledge@mit.edu (G. C. Rutledge).

1. Abstract

A kinetic model is proposed to describe the structure and rate of advancement of the growth front during crystallization. Solidification occurs through the mechanisms of surface nucleation and lateral spreading of the solid phase within layers in the vicinity of the growth front. The transformation from liquid to solid within each layer is described by an equation similar to the two-dimensional variant of the Johnson-Mehl-Avrami (JMA) equation, but in which the finite size and shape of the critical nucleus and the dynamic evolution of the solid fraction of the underlying layers are taken into account. Connection to the Regime theory of Hoffman and co-workers, for surface nucleation and spreading in one or two dimensions, is also made. Given only molecular level information regarding surface nucleation rates, lateral spreading rates and critical surface nucleus geometry, the resulting set of coupled nonlinear equations for solidification in each layer is numerically integrated in time to obtain the structure and rate of advancement of the growth front, for arbitrarily large systems and long times. Using this kinetic model with input parameters obtained from molecular dynamics simulations, a multi-scale modeling analysis of crystal growth in *n*-pentacontane (C50) is performed,.

for Table of Contents use only

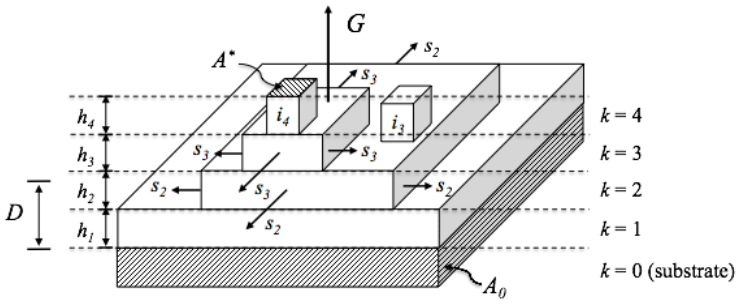

"Kinetic model for layer-by-layer crystal growth in chain molecules"

Alexander Bourque, Gregory C. Rutledge

2. Introduction

In the first paper of this series[1], we report a study of crystal growth from the melt of n-pentacontane (C50) by molecular dynamics simulation. Using a mean first passage time analysis, the distinct rates of surface nucleation and spreading within a molecular layer at the crystal growth front were quantified as functions of temperature, along with the size and shape of the critical surface nucleus. However, given current computational limitations, such simulations were limited to just enough layers (n=9) to observe steady state propagation of the growth front away from the substrate. In order to describe bulk crystallization of C50, a kinetic model is required that employs as input parameters the kinds of quantities that can be estimated by atomistic simulations and whose structure is consistent with the nature of crystal growth revealed by the atomistic simulations.

A logical starting point for modeling the crystallization of chain molecules like C50 is the surface nucleation model of Lauritzen and Hoffman (LH), first proposed to explain the growth of lamellar crystallites in polymers and the temperature dependence of the lamellar thickness.[2,3] According to LH theory, propagation of the crystal growth front proceeds in two steps: (1) an activated surface nucleation event in which one or a few chain stems attach within a molecular layer at the crystal growth front, and (2) lateral, one-dimensional (1D) spreading of the surface nucleus through the addition of more chain stems. Subsequent development of the model[4,5,6] was undertaken to account for the existence of three regimes, depending upon the relative rates of surface nucleation and spreading (to distinguish Regimes II and III) and whether the underlying substrate is sufficiently small to witness only one or a few nucleation events within a layer at the given rates (to distinguish Regimes I and II). Regime I is consistent with experimental observations in polymers at shallow supercoolings (up to $\Delta T=T_m-T_c$ of about 17°C, or $\Delta T/T_m \sim 0.12$ for polyethylene[5]), where the nucleation rate is relatively slow and the spreading rate is sufficiently fast that a single nucleation event is sufficient to cover the substrate. Regime II is observed for deeper supercoolings, where the nucleation rate is fast enough relative to spreading and substrate size

that multiple nucleation events occur within a layer. Regime III was incorporated into LH theory significantly later, to explain experimental observations[7] observed at still deeper supercoolings ($\Delta T/T_m$>0.16 for polyethylene[6]), where the nucleation rate is relatively fast and spreading is slow so that multiple nucleation events occur within a layer and on multiple layers simultaneously. LH theory and the existence of these three regimes of growth are supported by experimental observations in numerous polymer systems[8,9,10]. The details of the original model have been debated since its conception;[11,12] nevertheless, the concept of surface nucleation remains fundamental to many of the prevailing theories. LH theory provides analytical equations for crystal growth as functions of nucleation rate and spreading rate in each of the three regime limits; it does not attempt to describe quantitatively the crystal growth rate within the transitions between regimes. Importantly, because it assumes from the outset that chain segments deposit as entire stems, the LH model is inherently 2D, and it does not consider the structure of the critical nucleus explicitly. In contrast to this, molecular dynamics simulations of C50 indicate that the critical surface nucleus comprises about 20 CH_2 groups, much shorter than the final extended chain length in the crystal, and that it spreads nearly isotropically in both surface dimensions.[1] Numerous on-lattice Kinetic Monte Carlo simulations, in which individual segments or entire stems were added or subtracted at the growth front according to assumed kinetics, have been performed.[13,14,15,16,17]. The earliest of these models were generally of the type called "solid-on-solid" (SOS), in which solid material can deposit only upon solid material in the underlying substrate.[18] These simulations have allowed critical examination of many of the conditions inherent to LH theory, but have not resulted in significant revisions to the analytical form of the theory.

An alternative approach is that used to describe crystallization kinetics in bulk systems, including polymers. The equations for overall crystallization kinetics were proposed initially by Kolmogoroff[19] and developed concurrently by Avrami[20,21,22] and by Johnson and Mehl[23]. An alternative approach by Evans[24] led to similar equations. In this approach, nucleation events are typically distributed randomly at the onset of crystallization ("instantaneous nucleation") or are assumed to develop at a certain rate ("spontaneous

nucleation") within a volume V_o of untransformed (i.e. molten) material; a formulation of the model capable of treating temporally random nucleation events has also been presented[25,26]. The subsequent growth of these stable clusters in one, two or three directions gives rise to volumes (i.e. rods, disks or spheres, respectively) of transformed (i.e. solid) material that grow to impingement. In one of its more general forms, the Johnson-Mehl-Avrami (JMA) equation describing $X_V(t)$, the fractional volume $V(t)$ of transformed material at constant temperature, can be written as follows:[25]

$$X_V(t) = \frac{V(t)}{V_0} = 1 - \exp\left(-C\pi \int_0^t F(t') \left[\int_{t'}^t G(s)\, ds \right]^n dt' \right). \qquad (1)$$

Here $F(t)$ and $G(t)$ are the (constant or time-varying) nucleation and growth rates, respectively. The parameters C and n may assume values indicative of the different modes of nucleation – e.g. instantaneous or spontaneous – and the growth dimensionality. In this form, Eq. (1), the transformed volume associated with a nucleation event is assumed to be negligible. It is usually assumed that the sample volume V_0 is fixed and the growth rate $G(t)$ does not depend on the extent of transformation. Reviews of this method are available.[27,28] The JMA equation can be applied generally to a variety of phenomena (e.g. phase change, degradation, fracture, explosion, etc.)[25] and thus enjoys a wide range of applications.

Intermediate between these two well-known approaches is a layer-by-layer model in which the sequential transformation of each layer is modeled using a 2D JMA equation. Such an approach has been used by Bauer,[29] Kashchiev, [30] and Dubrovskii[31] to describe the deposition of crystals and thin films on substrates. In these models, the deposition of material on the substrate forms the first layer; further deposition of material upon the first layer forms a second layer, and so on for third and subsequent layers, as the film thickens. This pattern of growth has been called "layered growth", to distinguish it from "dislocation growth" or "spiral growth", in which deposition occurs at the leading edge of a screw dislocation and the film thickens without the formation of discrete layers[32]; the classical theories of crystal growth in

polymers are of the "layered growth" type. Importantly, in these models the substrate upon which the first layer forms may be a foreign surface, but subsequent layers of the depositing material nucleate and spread upon substrates comprising like material. Unlike the usual JMA theory where the initial volume V_0 (or area A_0 in 2D) is fixed for purposes of the entire transformation process, in this layer-by-layer approach A_0 is fixed only for the first layer; in all subsequent layers the kinetics of film deposition (or solidification) depend not only on the unsolidified area of that layer, but also on the solidified area of the layer upon which it deposits, both of which vary dynamically in time. The result is a model of the SOS type that comprises a set of coupled nonlinear equations. These equations have been solved analytically for a few particular cases[30,31], but more general examinations of deposition kinetics again resorted to Monte Carlo simulations.[33,34]

The crystallization of polymers and other materials is often accomplished with the aid of additives. Such additives may be dispersed molecularly or as particles of some finite size, and act as nucleating agents to enhance or otherwise modify crystallization kinetics or the morphology of crystallized material. In JMA theory, such nucleating agents are typically assumed to be infinitesimally small compared to V_0, and their action is taken into account through the nucleation kinetics[20,21]. Compared to the scale represented by a molecular simulation, however, even particulates as small as a few 100's of nm are more appropriately treated as foreign surfaces upon which nucleation occurs heterogeneously; the surface lowers the activation barrier for nucleation, so that heterogeneous nucleation of surface clusters occurs in preference to or in addition to homogeneous nucleation of primary clusters within the bulk. For heterogeneous nucleation occurring on the surface of a foreign particle, the analogy to layered growth is apparent.

In this work, we derive the layer-by-layer kinetic model for crystallization from a foreign substrate into the melt by adapting the derivation for kinetics of crystallization by Johnson and Mehl.[23] In particular, crystal growth away from a substrate is modeled as the coupled evolution of crystallinity within distinct, 2D molecular layers. Consistent with molecular level simulations, the size of the critical surface nucleus

is allowed to be finite, and the subsequent spreading of that cluster may occur in either one or both directions within a layer. At this stage, chain connectivity is only implied; one of the directions is assumed to be that of the chain axes, but neither full extension of the chain nor chain folding are taken explicitly into account. Nevertheless, this treatment is consistent with our observations of crystallization of C50 by molecular dynamics,[1] where chain connectivity is fully respected, and full extension occurs only in the latest stages of layer completion. This kinetic model is shown to reproduce Regime II and Regime III behavior of LH theory, as well as their dependence on critical nucleus size and spreading dimensionality. Additionally, a mean "roughness" of the growth front is calculated, and its behaviors in Regimes II and III are shown to be consistent with the results of Monte Carlo simulations by Guttman and Dimarzio.[13] Unlike the local measure employed by Guttman and DiMarzio, however, the mean roughness of the growth front calculated here could be amenable to experimental verification. Lastly, we apply this model to the case of C50 crystallization, using parameters obtained directly from molecular dynamics simulations.[1] To our knowledge, this is the first demonstration of a multi-scale (atomistic-continuum) model for crystallization of chain molecules.

3. Theory

The kinetic theory developed here describes the layer-by-layer growth of a solid phase from a supercooled (or supersaturated) liquid with the aid of a substrate, which may be either the same as or different from the solid phase that forms upon it. For simplicity, the model assumes that the initial substrate surface is flat, with area A_0, at time $t = 0$. The layers of solid that form upon the substrate are indexed by $k = 1, 2, 3, \ldots k_{max}$ as shown in Figure 1 with each layer $k - 1$ serving as the substrate for the next layer, k. In accord with the LH model, we envision these layers to be molecularly thin, with thicknesses h_k. Any substrate of finite size $R >> h_k$ should be well approximated by the flat surface employed here. Solidification occurs through propagation of the solid-liquid interface into the supercooled liquid and the accompanying growth of the solid phase at the expense of the liquid.

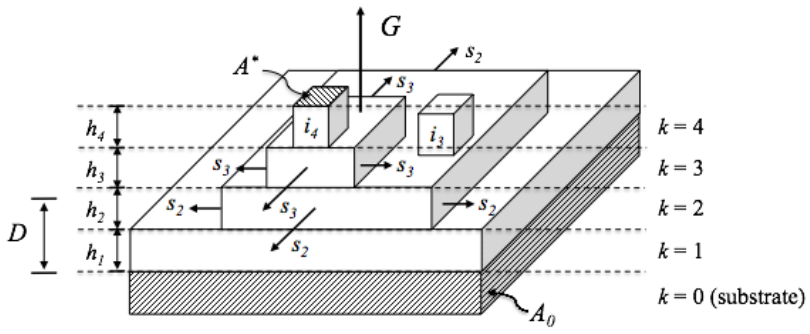

Figure 1. Schematic of layer-by-layer solid growth from a supercooled liquid phase atop a substrate of area A_0. Deposition in one or two dimensions occurs through nucleation of new clusters of area A^* in each layer at a rate i_k, and through spreading of existing clusters in each layer at a rate s_k. Each layer has a constant thickness h_k. At any instant in time, the effective position of the growth front (D) can be measured. Propagation of the growth front occurs at a rate $G=dD/dt$.

Propagation or growth of the solid phase is made possible by the formation of pseudo-two dimensional surface nuclei randomly on the substrate layer $k - 1$, followed by spreading of such nuclei within the layer k. In accord with the idea of "solid-on-solid contact", surface nuclei can only form on a substrate layer that has attained a sufficient solid fraction itself to support nucleation, and these nuclei can spread to be only as large as the underlying solid layer itself. In this regard, the kinetic model proposed here, like those of Kashchiev and of Dubrovskii, is similar to a two-dimensional variant of the JMA equation. However, since the area of the substrate layers themselves in layers $k > 0$ evolve with time, the area of material available for solidification is dynamic, and may either increase or decrease with time, in contrast to V_0 of JMA theory. Consistent with our molecular level interpretation of the layer thickness, we consider the surface nucleus to be of finite size A^*.

To begin, one can write the following equation for the differential change in area of a section of solid material within a layer:

$$dA = br^{\alpha} dr \,, \tag{2}$$

where A is the area of a solid section within a layer, r is the characteristic size of the growing solid section, and α and b are parameters that depend upon the dimensionality of spreading within the layer. For isotropic radial spreading within a pseudo-two dimensional layer of material, $b = 2\pi$ and $\alpha = 1$. For the particular case adopted by LH theory, where the surface nucleus comprises a single, fully extended molecular stem, and spreading proceeds by the subsequent deposition in one dimension of adjacent, full length stems, $\alpha = 0$ and b is the lamellar thickness, ℓ .

The linear dimension at time t of a growing solid section that started at time τ as a surface nucleus of critical size r^* is given by $r = r^* + s(t - \tau)$ where s is the lateral spreading rate. The differential change in area thus has two contributions, one due to the creation of the critical nucleus and the other due to spreading of that nucleus to form a cluster. The differential change in area is thus evaluated piecewise. At any time t, the contribution due to new nuclei that form at time $\tau = t$ is

$$dA^{(n)} = b\left(r^*\right)^{\alpha+1} \delta(t-\tau) \,, \tag{3}$$

while the contribution due to spreading of older clusters that formed at any $\tau < t$ is

$$dA^{(s)} = bs\left[r^* + s\left(t-\tau\right)\right]^{\alpha} dt \,. \tag{4}$$

The nucleation of such solid sections in layer k depends on the area of solid material in its substrate layer $k - 1$. For this purpose, one can write

$$dn_k = i_k A_{k-1}(\tau) d\tau \,, \tag{5}$$

where dn_k is the number of nuclei formed in layer k in a short time interval $d\tau$ at time τ, i_k is the surface nucleation rate in layer k and $A_{k-1}(\tau)$ is the solid area in layer $k - 1$ at time τ. The total change in solid area within layer k in the interval dt can then be written as follows:

$$
\begin{aligned}
dA_k^I &= \left[dA^{(n)} + dA^{(s)} \right] dn_k \\
&= \left\{ b_k i_k A_{k-1}^I(t) \left[r_k^* \right]^{\alpha_k + 1} + \int_{t_{0,k}}^{t} b_k i_k s_k A_{k-1}^I(\tau) \left[r_k^* + s_k (t - \tau) \right]^{\alpha_k} d\tau \right\} dt
\end{aligned}
\tag{6}
$$

Here, the integral on the right hand side accounts for the cumulative spreading of all clusters that nucleated at any time $t_{0,k} < \tau < t$, where $t_{0,k}$ is the first time point at which the solidification in layer $k - 1$ is sufficient to support a nucleation event in layer k. The superscript Roman numeral I has been introduced to distinguish the total extended solid area within a layer k from that of the individual solid sections that it comprises. Thus, a layer may solidify by multiple surface nucleation events, by spreading of clusters to fill the layer, or a combination of both. The subscript k introduced for parameters b, α, s, i and r^* permits distinct kinetics for each layer k. For growth front propagation in a crystallizing polymer melt, the distinction is unnecessary because all layers exhibit the same characteristic molecular rates. However, for crystallization near a foreign substrate, crystal lattice mismatch and differences in surface energies between the substrate and the depositing phase leads to layer-dependent molecular parameters.

Following the approach of Johnson and Mehl[23], we next introduce $U_k(t)$, the fraction of untransformed material remaining within layer k that is adjacent to solid substrate in layer $k - 1$ at time t, within which additional surface nucleation and spreading is possible:

$$
U_k(t) = \frac{A_{k-1}^I(t) - A_k^I(t)}{A_{k-1}^I(t)} \,. \tag{7}
$$

Then, $U_k(t)$ is used to reduce the differential change in total "extended" area within layer k by an amount proportional to the untransformed fraction, to obtain the differential change in the actual area of solidified material:

$$dA_k^{II} = U_k(t)dA_k^I$$
$$= b_k i_k U_k(t)\left[A_{k-1}^I(t)\left[r_k^*\right]^{\alpha_k+1} + s_k \int_{t_{0,k}}^{t} A_{k-1}^I(\tau)\left[r_k^* + s_k(t-\tau)\right]^{\alpha_k} d\tau \right] dt \quad (8)$$

Here, the superscript Roman numeral *II* has been introduced to distinguish the differential change in actual area from that of the extended area, which only takes into account the dynamical evolution of the substrate.

Given the set of parameters b, α, s, i, r^* and the initial substrate area A_0, a set of equations of the form of Eq. (8) for $k = 1, 2, 3\ldots k_{max}$ can be numerically integrated in sequence. That is, Eq. (8) can be integrated forward one time step for $k = 1$ followed by integration for $k = 2, 3$, and so on, because the rate of solidification dA_k/dt of layer k depends on the solid area in layer $k - 1$. MATLAB R2015a version 8.5 was used to perform the integrations, using the routine `ode45`. Throughout this work, $t_{k,0}$ was set to the time at which $A_{k-1}^{II} = A^* = b\left(r^*\right)^{\alpha+1}$.

Once the functions $A_k^{II}(t)$ have been determined, the total fraction of transformed material in layer k, $X_k(t)$, can be expressed relative to the original substrate area A_0 using the relation,

$$X_k(t) = \frac{A_k^{II}(t)}{A_0} \quad (9)$$

The average displacement $D(t)$ of the solidification front is then,

$$D(t) = \sum_{k\geq 1} h_k X_k(t) \quad (10)$$

The propagation of the solidification front, or growth rate $G(t)$ is expressed by

$$G(t) = \frac{dD(t)}{dt} \quad (11)$$

It can be verified that the instantaneous displacement of the interface, $D(t)$, as expressed in Eq. (10) is numerically equivalent to the location of a Gibbs dividing surface that identifies the crystal-amorphous

interface. The discrete summation of the differences between the true crystallinity profile and the Gibbs dividing surface for each layer vanishes when the step function is located at $z_k = D(t)$:

$$X_{c,\text{int}} = \sum_k \left[H(D(t) - z_k) - X_k(t) \right] h_k = 0 \qquad (12)$$

where $z_k = \sum_{j=1}^{k} h_j$ is the height of layer k, X_k decreases with increasing k, and $H(x)$ is the Heaviside step function. The squared roughness $R^2(t)$ of the crystal growth front at time t is then defined using the analogue of Eq. (12) that computes the distance-weighted deviation of the growth front from its mean position, as follows:

$$R^2(t) = \sum_k \left[H(D(t) - z_k) - X_k(t) \right] \left[D(t) - z_k \right] h_k \qquad (13)$$

Finally, we note that solution of the model for fixed A_0 yields layer-dependent behavior for the first few layers close to the initial substrate at $k = 0$, which we call the "near surface" behavior. This behavior holds even if the parameters of the model (h, b, α, s, i, r^*) are layer-independent, because only for layer $k = 1$ is $A_{k-1} = A_0 =$ constant. For studies of heterogeneous nucleation, "near surface" behavior is also of great importance, but in such cases, the values (h_k, b_k, α_k, s_k, i_k, r_k^*) are expected to be vary with layer number for small values of k.

4. Model Results

4.1 General behavior of the model

Here we consider only the simplest case, in which the substrate in contact with a supercooled melt is the solid phase of the same material. In this case, the kinetic parameters h_k, b_k, α_k, s_k, i_k and r_k^* have no layer dependence; henceforth, the subscript k is dropped. Figure 2a shows the fraction of transformed material for the first several layers adjacent to a substrate of fixed area A_0 under the conditions where the critical nucleus size is negligible and clusters spread isotropically. The shape of each X_k(t) profile for $k > 1$ is

nearly unchanged from the profile in the first layer, X_1(t). For $k \geq 6$, the curves are identical except for a constant time shift, representative of the waiting period between nucleation events in adjacent layers.

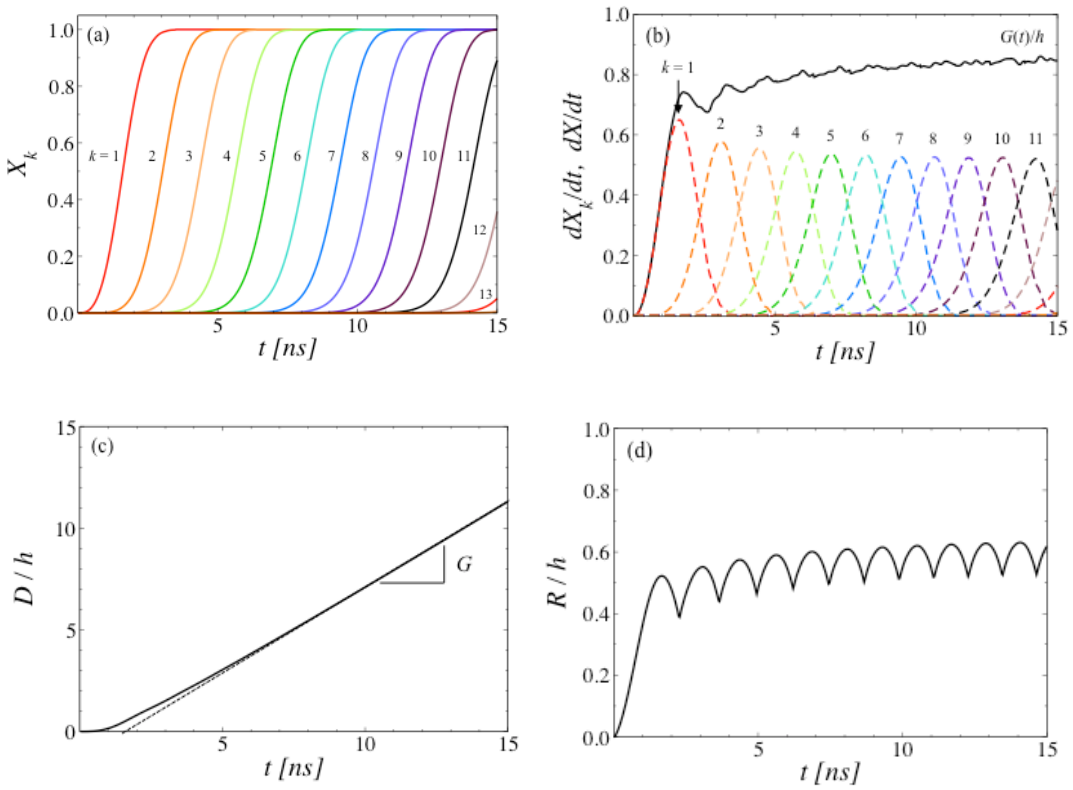

Figure 2. (a) Layer-by-layer transformation, (b) rate of crystallization $dX_k/dt(t)$ within each layer and total rate of crystallization $dX/dt(t)$ shown as the solid line, (c) displacement of the crystal growth front, and (d) surface roughness for a material crystallizing on its own substrate, for fixed area $A_0/h^2 = 1000$ for $r^* = 0$, $\alpha = b = 1$ and $s/h = ih^2 = 1$ ns^{-1}.

Figure 2b shows the rate of crystallization dX_k/dt within each layer, as well as the total rate of crystallization,

$$dX/dt = \sum_{k\geq 1} dX_k/dt = G(t)/h \qquad (14)$$

.

The rate of conversion from melt to solid in each layer passes through a maximum, first increasing as both the area available in the underlying layer and the number of nuclei grow, then decreasing as the remaining fraction of untransformed material in the layer becomes depleted. From the heights of the maxima, it is evident that the rate of crystallization is fastest in the first layer (k = 1), since the entire area of the substrate is immediately available to support surface nucleation and spreading in this layer. However, crystallization becomes significant in layer k = 2 already when layer 1 is only about 30% crystallized; crystallization becomes significant in layer 3, when layer 1 is about 90% crystallized. Since the total crystallization rate is the sum of the crystallization rates in each layer, the total crystallization rate is slow initially, but increases to a steady state value by 10 ns as multiple layers become involved.

Another way to examine the rate of crystallization is through the displacement $D(t)$ of the crystal growth front, shown in Figure 2c. As indicated by Eq. (11), the slope of this curve gives the growth rate $G(t)$. In accord with Figure 2b, propagation of the growth front is initially slow for small k, but increases to a constant value, G, within about 10 ns. The dashed line in Figure 2c illustrates the condition where growth is constant. This condition reflects the self-similarity of crystallization for each layer, which was observed for layers $k \geq 6$ in Figure 2a.

Figure 2d shows the instantaneous surface roughness $R(t)$. Starting at t = 0, the roughness increases rapidly, but passes through a local maximum within the first 2 ns. From Figure 2a, it is clear that the dynamics of surface roughening in the first 2 ns are dictated by the dynamics in layer k = 1. In the absence of a second layer growing atop the first, Eq. (13) predicts that roughness would go through a maximum when X_1 = 0.5, and approach R = 0 as the layer reaches completion. In reality, this behavior is avoided because layer k = 2 starts to crystallize around 1 ns, and the roughness increases again, eventually

leveling off by 10 ns at a roughness around $R/h = 0.6$. The oscillatory behavior of $R(t)$ versus time is an artifact of the discrete nature of the layer-by-layer summation in Eq. (13) while $D(t)$ varies continuously.

Figure 3a shows the fraction of transformed material for the first several layers under the conditions where the nucleation rate is $ih^2 = 10^4$ ns^{-1}, several orders of magnitude greater than in Figure 2. Under these conditions, the crystallization behavior is qualitatively different from that in Figure 2. The profiles of X_k at large k are no longer merely shifted in time, but instead become increasingly broad with increasing layer number k. Similarly, Figure 3b shows the rate of crystallization dX_k/dt within each layer, as well as the total growth rate, $G(t)/h$. Whereas the total growth rate rapidly reaches steady state, the rate of transformation within the individual layers varies significantly with layer number k. dX_i/dt decays exponentially from a peak at $t = 0$, while the peak transformation rate in subsequent layers decreases with increasing layer number k, and the number of layers actively contributing to the overall growth rate increases with time.

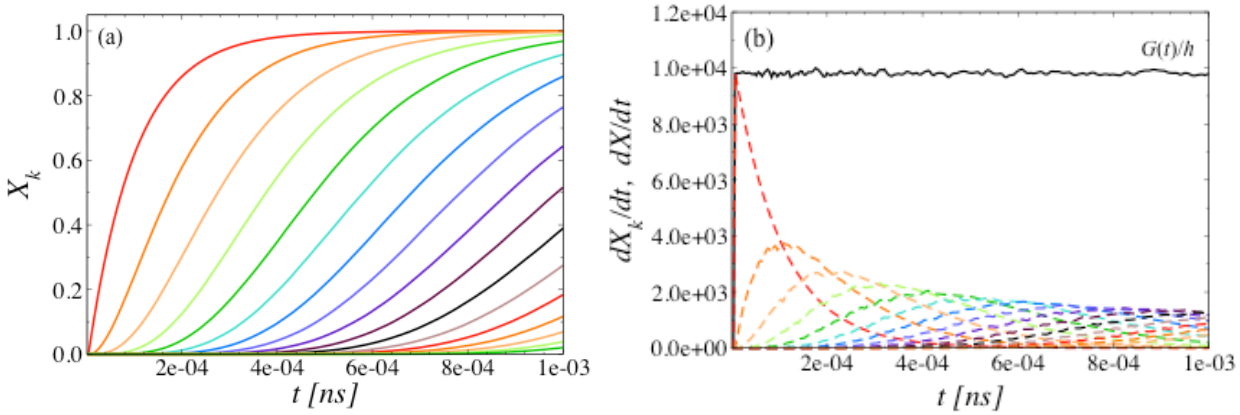

Figure 3. (a) Layer-by-layer transformation, (b) rate of crystallization $dX_k/dt(t)$ within each layer and total rate of crystallization $dX/dt(t)$ shown as the solid line for fixed substrate area A_0 for $r^*/h = 1$, $\alpha = b = 1$, $s/h = 1$ ns^{-1} and $ih^2 = 10^4$ ns^{-1}.

Figure 4 shows the growth rates G as functions of the constituent parameters s, i and r^*. Results are presented for both 1D ($\alpha = 0$) and 2D (isotropic, $\alpha = 1$) spreading. In Figure 4a, the growth rate is shown to increase monotonically with spreading rate s. That is, for a given surface nucleation rate, a fast spreading rate increases the available area upon which the next layer can crystallize and therefore leads to an increase in the overall growth rate. However, one observes a distinctive difference in the slope of $\log_{10}G$ versus $\log_{10}s$ for low and high values of the spreading rate, s, and for different values of α; similar differences are apparent for the slopes of $\log_{10}G$ versus $\log_{10}i$ (Figure 4b) and $\log_{10}r^*$ (Figure 4c). From these slopes, one readily deduces the existence of two regimes, for both $\alpha = 0$ and $\alpha = 1$. For $\alpha = 0$, corresponding to the conditions prevailing in the LH theory, one regime scales as $G \sim (is)^{1/2}$ and can immediately be identified as Regime II, where s is relatively large and i is relatively small. The other regime scales as $G \sim (ir^*)$, and can be identified as Regime III for relatively small s and large i or r^*. In this regime, growth occurs primarily through the accumulation of multiple nucleation events occurring simultaneously on multiple layers. Significantly, this regime is not obtained unless the finite size r^* of the nucleus is taken into account. In the conventional LH theory and its variants, r^* is identified with the width of one or a few molecular stems, whereas in JMA theory r^* is usually assumed to be negligible. In a multi-scale model, however, r^* (and α) is dictated by an appropriate analysis of the molecular level simulation. The transition from Regime II to Regime III is marked by the condition $\left(iA^*\right)\Big/\left(s/r^*\right) \approx 1$, where $A^*=br^*$. Using the same regime notation for the 2D case ($\alpha = 1$), one obtains $G \sim (is^2)^{1/3}$ in Regime II and $G \sim (ir^{*2})$ in Regime III. The alternate scaling with spreading rate in Regime II is consistent with the change from 1D to 2D spreading. The alternate scaling with critical nucleus size in Regime III is indicative of deposition of disk-like nuclei in lieu of rod-like stems. The transition from Regime II to Regime III in 2D is again marked by the condition $\left(iA^*\right)\Big/\left(s/r^*\right) \approx 1$, where now $A^*=br^{*2}$.

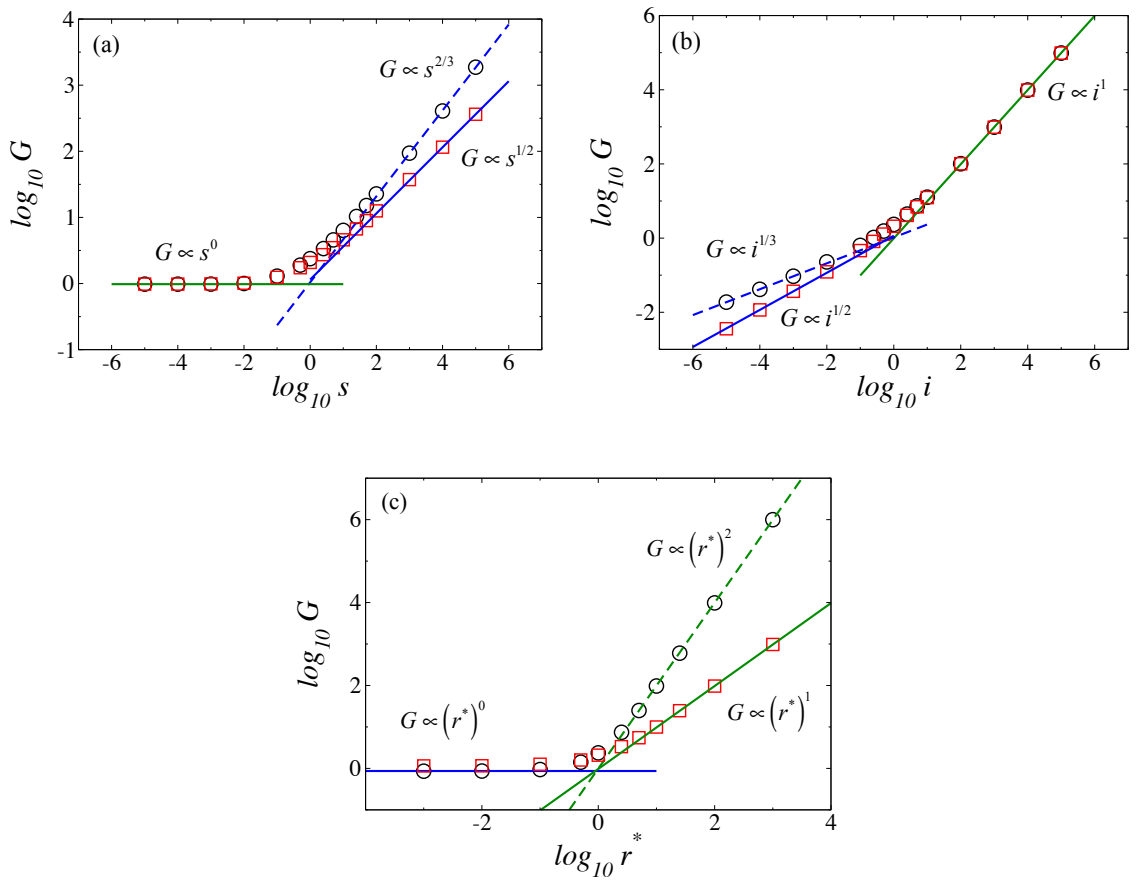

Figure 4. Growth rate G/h from a surface of identical material with fixed area A_0/h^2, plotted as function of (a) spreading rate s/h, (b) surface nucleation rate ih^2 and (c) critical nucleus size r^*/h. Kinetic modeling results are shown for $\alpha = 0$ (red squares) and for $\alpha = 1$ (black circles). For each value of α, two limiting behaviors are observed for G as a function of the parameters s, i and r^*, respectively. For $\alpha = 0$ (solid lines) and $\alpha = 1$ (dashed lines), these limiting behaviors are identified as Regime II (blue lines) and Regime III (green lines). In all cases, $b = 1$, $h = 1$ and, unless stated otherwise, $r^*/h = 1$, $s/h = 1$ ns^{-1}, $ih^2 = 1$ ns^{-1}.

It is worth noting that the Regime I of LH theory is not observed under any circumstances in Figure 4, including variations of A_0 down to the lower bound of A^*. Regime I, which occurs in polymers at the shallowest supercoolings, has been postulated to occur under conditions of large spreading rate s and

relatively small substrate size A_0. We expect the transition from Regime II to Regime I to occur in the vicinity of $\left(iA_0\right)\Big/\left(s/r^*\right)\approx 1$. Under such circumstances, only one or a few nucleation events, followed by relatively rapid spreading, may be sufficient to completely solidify a single layer with high probability before the next layer is initiated. This limit appears to be inconsistent with the assumption of a constant nucleation rate *i*, invoked in Eq (5). We speculate that a stochastic treatment of nucleation rate may be necessary to capture Regime I and its transition from Regime II. However, such analysis is beyond the scope of the current work.

Figure 5 shows the scaled roughness *R/h*, given by Eq. (13), for surface nucleation rates spanning several orders of magnitude, spanning Regime II and Regime III. The time scales are significantly different for such a broad range of surface nucleation rates, so the time axis is scaled by the growth rate *G*. For behavior characteristic of Regime II (e.g. $ih^2 < 0.1$ ns^{-1}), the scaled roughness attains a steady state value $R/h < 1$ after the deposition of about 5 to10 layers. This steady state value corresponds to only one or two molecular layers actively crystallizing at the growth front at any given time. For faster nucleation rates (or slow spreading rates), as the system approaches the transition from Regime II to Regime III, one observes a transition from roughness at the growth front characterized by a time-independent *R/h* to one characterized by a time-independent *d(R/h)/dt*. That is, for behavior characteristic of Regime III (e.g. $ih^2 > 10$ ns^{-1}), *R/h* increases approximately linearly with scaled time after the deposition of about 5 to 10 layers, and grows without bound. This behavior is consistent with that observed by Guttman and DiMarzio using a Kinetic Monte Carlo simulation with spreading in 1D.[13]

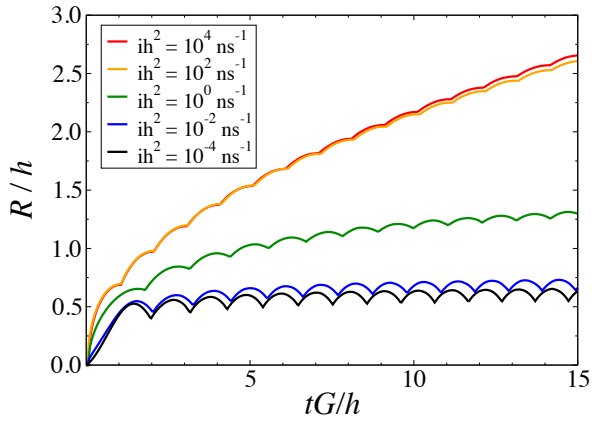

Figure 5. Surface roughness R/h as a function of time (scaled by G/h) for a range of surface nucleation rates spanning Regimes II and III. Results are presented for 2D spreading (isotropic, $\alpha = 1$); similar results were obtained for 1D spreading ($\alpha = 0$). In each R/h profile $b = 1$, $r^*/h = 1$ and $s/h = 1$ ns^{-1}.

4.2 A multi-scale model of crystal growth

In this section we apply our kinetic model to the description of crystal growth of n-pentacontane ($C_{50}H_{102}$, or C50 for short) from the melt. In the first paper of this series[1], the results from molecular dynamics (MD) simulations for crystallization of C50 from the melt state upon a polyethylene (PE) substrate were presented. Methods for the determination of the crystal growth rate, G, as well as for the various layer-dependent parameters of the kinetic model (b_k, α_k, s_k, i_k, r_k^*) were reported, and values were obtained for crystallization of C50 as fully extended chain crystallites. For layers $k \geq 4$, it was determined that these parameters become more or less layer-independent, thereby identifying the "far from surface" behavior typical of C50 crystallization. Layer-independent values of s and i were obtained for isothermal crystal growth at temperatures from 300 to 370 K (the equilibrium melting point T_m of C50 based on the force field used in that work); these values are reproduced in Table 1. The 2D nucleus was observed to exhibit nearly isotropic, radial growth; thus $b = 2\pi$ and $\alpha = 1$ were employed here for kinetic modeling purposes. The size of the critical surface nucleus was found to be $n^* = 20$ CH_2 monomers, corresponding to a critical area $A^* = 1.29$ nm^2 and $r^* = 0.64$ nm. Based on the size of those simulations, $A_0 = 42$ nm^2 (i.e. $A_0/A^* \sim 33$).

The layer thickness was h=0.4 nm. According to Table 1, crystal growth for C50 is estimated to be in Regime III or in the vicinity of transition to Regime II over the entire range of temperature, based on the simulation data.

Table 1. Surface spreading rate s and surface nucleation rate i at the growth front of a C50 crystal crystallizing at temperature T_c, measured by molecular dynamics simulation.[1] Also tabulated are the criteria for transitions from Regime II to either Regime III or Regime I, and the rate at which the growth surface roughness increases in Regime III, estimated by both the kinetic model and the molecular simulations.

T_c (K)	s (nm ns^{-1})	i (nm^{-2} ns^{-1})	$\left(iA^*\right)/\left(s/r^*\right)$	$\left(iA_0\right)/\left(s/r^*\right)$	$d(R/h)/dt_{kinetic}$ (10^3 ns^{-1})	$d(R/h)/dt_{sim}$ (10^3 ns^{-1})[(a)]
300	0.019	0.054	4.74	77.1	4.1	8.5
320	0.028	0.053	3.16	50.4	4.0	11
340	0.046	0.052	1.89	30.7	1.9	10
360	0.055	0.052	1.58	25.7	1.6	3.2
370	0.051	0.052	1.70	27.7	1.4	3.4

[(a)] estimates based on linear fit to last 10 ns of simulation time, from Ref 1.

Figure 6 shows the growth rate G predicted by the kinetic model described here, using the spreading and surface nucleation rates obtained from MD simulation at each temperature. For comparison, the growth rates obtained by tracking the midpoint of the growth front during MD simulations of C50 crystallization are also shown in Figure 6. The growth rates predicted by the kinetic model are 2-4 times higher than those measured directly by MD simulation. As discussed in the companion paper,[1] the finite size of the MD simulations results in frustration of crystallization as the layers near completion, due to the presence of periodic boundaries, and gradual attrition of the growth front. Such frustration, and the finite size effect that gives rise to it, are completely avoided in the kinetic modeling approach presented here. Thus, the kinetic model yields a higher growth rate that is arguably more representative of a macroscopic system undergoing crystallization.

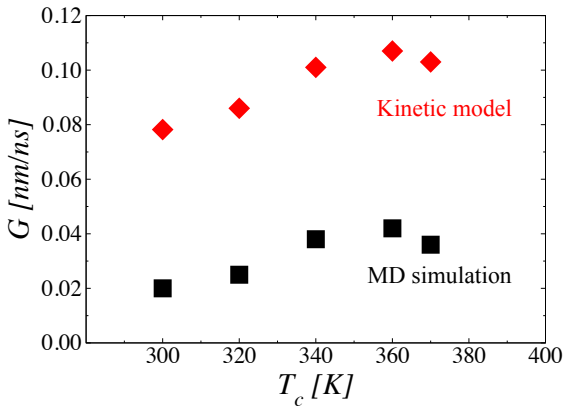

Figure 6. Growth rate *G* of C50 measured by molecular dynamics simulation (black squares) and predicted by the kinetic model (red diamonds)

Figure 7 shows the scaled roughness *R*/*h* predicted by the kinetic model using the parameters and rates from MD simulation of C50 crystallization. The resulting roughness profiles are remarkably similar to those obtained from analysis of the simulation (*c.f.* Figure 10 of Ref 1). The magnitudes of *R*/*h* and their tendency towards continued increase at the lower temperatures provide additional evidence that the crystallization of C50 is in Regime III or in the vicinity of transition to Regime II. Appropriate to Regime III, the values of *d(R/h)/dt* determined by the kinetic model and by molecular simulations are compared in Table 1. The simulation results are rather noisy, but both methods suggest that roughness at the growth front increases with decreasing temperature.

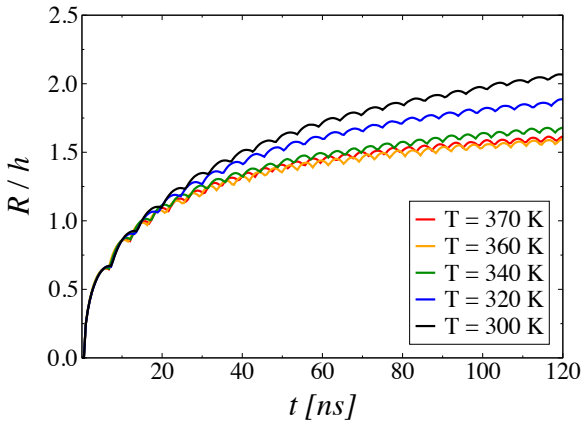

Figure 7. Scaled roughness R/h at the growth front of crystallizing C50 predicted by the kinetic model.

Both surface spreading and surface nucleation are molecularly fast processes. Their time scales do not readily permit their direct measurement by experiment. Molecular simulation offers a means for direct observation of these molecular rates, albeit *in silico*. However, molecular simulations alone cannot be used to model crystal growth over more than a few hundreds of nanoseconds, with current technology. Simulation times scale with the number of atoms, making it impractical to simulate increasingly large systems. The kinetic model presented here respresents an important part of a multi-scale modeling strategy that serves to bridge the gap between molecular processes and the macroscopically observable growth rate.

5. Conclusions

The method presented here offers one approach to modeling crystallization from a substrate with area A_0 into a supercooled melt. Features of the approach include layer-by-layer deposition of solid material on previously solidified portions of the underlying layers, in a type of solid-on-solid model. Critical surface nucleus size, surface nucleation rate, and spreading rate within each layer are the essential constitutive parameters of the model. Estimates of these constitutive parameters as functions of temperature may be

based on classical nucleation theory, physical models such as reptation in polymer melts, or obtained directly by experiments or molecular simulations. Coupled solution of the equations for evolution of the solid fraction within each layer makes the method more robust than analytical solutions that can be obtained in certain limiting cases, allowing one to model growth behavior in different regimes as well as in the vicinity of transitions between regimes seamlessly. Meanwhile, the method is computationally more efficient than a Kinetic Monte Carlo simulation. The method is shown to reproduce important aspects of Regime growth from LH theory for polymer crystallization in specific cases, but is not limited to such cases. It is also shown to reproduce important features of the growth front, such as surface roughness, previously estimated by Monte Carlo simulations.

Using molecular dynamics simulations to estimate the essential constitutive parameters (s, i, r^* and α) over a wide range of temperatures in combination with the kinetic model described here to model layer-by-layer growth for arbitrary values of A_0 and number of layers, one obtains a multi-scale modeling strategy for characterizing crystal growth kinetics from first principles. In combination with the companion paper, this strategy is demonstrated here for crystallization of n-pentacontane, but it should be generally applicable to a variety of materials for any supercooling and substrate size such that growth is consistent with Regime II or Regime III. Application of the method to more complex cases such as chain folded crystallization in polymers, especially that typical of Regime I, may require further refinements, but the method described here offers a reasonable starting point for such refinements. To our knowledge, this is the first time that chemically specific growth parameters (s, i, r^*, α) have been obtained by molecular simulation and then used to model directly the propagation of the growth front over long time and length scales using a continuum kinetic model.

6. References

(1) Bourque, A. J.; Locker, C. R.; Rutledge, G. C. Molecular dynamics simulation of surface nucleation during growth of an alkane crystal, (in preparation)

(2) Lauritzen, J. I.; Hoffman, J. D. Theory of formation of single polymer crystals with folded chains in dilute solution, *J. Res. Nat. Bur. Std. A*, **1970**, 64, 73.

(3) Hoffman, J. D.; Miller, R. L. Kinetic of crystallization from the melt and chain folding in polyethylene fractions revisited: theory and experiment, *Polymer*, **1997**, 38, 3151-3212.

(4) Lauritzen, J. I. Effect of a finite substrate length upon polymer crystal lamellar growth rate, *J. Appl. Phys.*, **1973**, 44, 4353-4359.

(5) Hoffman, J.D.; Frolen, L. J.; Ross, G. S.; Lauritzen, J. I. On the growth rate of spherulites and axialites from the melt in polyethylene fractions: Regime I and Regime II crystallization, *J. Res. Nat. Bur. Std. A*, **1975**, 79, 671-699.

(6) Hoffman, J.D. Regime III crystallization in melt-crystallized polymers: The variable cluster model of chain folding, *Polymer*, **1983**, 24, 3-26.

(7) Barham, P. J.; Jarvis, D. A.; Keller, A. A new look at the crystallization of polyethylene. III. Crystallization from the melt at high supercoolings, *J. Polym. Sci.*, **1982**, 20, 1733-1748.

(8) Armisted, J. P.; Hoffman, J. D. Direct of evidence of regimes I, II, and III in linear polyethylene fractions as revealed by spherulite growth rates, *Macromolecules*, **2002**, 35, 3895-3913.

(9) Cheng, S. Z. D.; Janimak, J. J. Crystal growth of intermediate-molecular-mass poly(ethylene oxide) fractions from the melt, *Polymer*, **1990**, 31, 1018.

(10) Cheng, S. Z. D.; Janimak, J.J.; Zhang, A.; Chang, H. N. Regime transitions in fractions of isotactic polypropylene, *Macromolecules*, **1990**, 23, 298-303.

(11) Frank, F.C.; Tosi, M. On the theory of polymer crystallization, *Proc. R. Soc. Lond A*, **1961**, 263, 323-339.

(12) Point, J. J. A new theoretical approach of the secondary nucleation at high supercooling, *Macromolecules*, **1979**, 12, 770-775.

(13) Guttman, C. M.; DiMarzio, E. A. Monte Carlo modeling of kinetics of polymer crystal growth: Regime III and its implications on chain morphology, *J. Appl. Phys.*, **1983**, 54, 5541-5552.

(14) Sadler, D. M.; Gilmer, G. H. Rate-theory model of polymer crystallization, *Phys. Rev. Lett.*, **1986**, 56, 2708-2711.

(15) Doye, J. P. K.; Frenkel, D. Kinetic Monte Carlo simulations of the growth of polymer crystals, *J. Chem. Phys.*, **1998**, 110, 2692-2702.

(16) Chen, C. M.; Higgs, P. G. Monte-Carlo simulations of polymer crystallization in dilute solution, *J. Chem. Phys.*, **1998**, 108, 4305-4314.

(17) Hu, W. Chain folding in polymer melt crystallization studied by dynamic Monte Carlo simulations, *J. Chem. Phys.*, **2001**, 115, 4395-4401.

(18) Leamy, H. J.; Gilmer, G. H.; Jackson, K. A. Statistical thermodynamics of clean surfaces. In *Surface Physics of Materials*; Blakely, J. M., Ed. Academic Press, Inc.; New York, **1975**, pp 121-188.

(19) Kolmogorov, A. N. K statisticeskoj teorii kristallizacii metallov. *Izvestiya Akademii Nauk SSSR*, **1937,** 3, 355–359.

(20) Avrami, M. Kinetics of phase change. I: general theory, *J. Chem. Phys.*, **1939**, 7, 1103-1112.

(21) Avrami, M. Kinetics of phase change II: transformation-time relations for random distribution of nuclei, *J. Chem. Phys*., **1940**, 8, 212.

(22) Avrami, M. Kinetics of phase change. III: granulation, phase change and microstructure, *J. Chem. Phys.*, **1941**, 9, 177-184.

(23) Johnson, W. A.; Mehl, R. F. Reaction kinetics in processes of nucleation and growth, *Trans. AIME*, **1939**, 135, 416–442.

(24) Evans, U. R. The laws of expanding circles and spheres in relation to the lateral growth of surface films and the grain-size of metals, *Trans. Faraday Soc.*, **1945**, 41, 365-374.

(25) Piorkowska, E.; Galeski, A. Growth sites in space and time, *J. Phys. Chem.*, **1985**, 89, 4700-4703.

(26) Piorkowska, E.; Galeski, A. Statistical development of spherulite patterns, *J. Polym. Sci.,* **1985**, 23, 1723-1745.

(27) Piorkowska, E.; Galeski, A.; Haudin, J-M. Critical assessment of overall crystallization kinetics theories and predictions, *Prog. Polym. Sci.*, **2006**, 31, 549-575.

(28) Piorkowska, E.; Galeski, A. Overall crystallization kinetics. In *Handbook of polymer crystallization*; Piorkowska, E., Rutledge, G. C., Eds.; John Wiley & Sons, Inc.; Hoboken, NJ, **2013**, pp 215-235.

(29) Bauer, E. Phänomenologische Theorie der Kristallabscheidung an Oberflächen. I, *Z. Kristallagor*, **1958**, 110, 372-394.

(30) Kashchiev, D. Growth kinetics of dislocation-free interfaces and growth mode of thin films, *J. Cryst. Growth*, **1977**, 40, 29-46.

(31) Dubrovskii, V.G. Nucleation and growth of absorbed layer, *Phys. Status Solidi*, **1992**, 171, 345-356.

(32) Burton, W. K.; Cabrera, N.; Frank, F. C. The growth of crystals and the equilibrium structure of their surfaces, *Phil. Trans. R. Soc. A*, **1951**, 243, 299.

(33) Kashchiev, D.; van der Eerden, J. P.; van Leeuwen, C. Transition from island to layer growth of thin films: a Monte Carlo simulation, *J. Cryst. Growth*, **1977**, 40, 47-58.

(34) Gilmer, G. H.; Huang, H.; de la Rubia, T. D.; Torre, J.D.; Baumann, F. Lattice Monte Carlo models of thin film deposition, *Thin Solid Films*, **2000**, 365, 189-200.